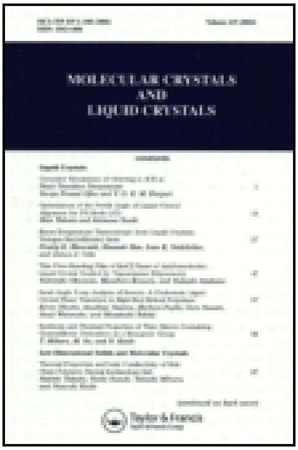

Molecular Crystals and Liquid Crystals

Publication details, including instructions for authors and subscription information:
http://www.tandfonline.com/loi/gmcl16

Physical Properties of Nematic Materials Containing Different Ring Systems

M. J. Bradshaw [a], D. G. Mcdonnell [a] & E. P. Raynes [a]

[a] Royal Signals and Radar Establishment, Malvern, Worcs, WR14 3PS, UK

Version of record first published: 14 Oct 2011.

To cite this article: M. J. Bradshaw , D. G. Mcdonnell & E. P. Raynes (1981): Physical Properties of Nematic Materials Containing Different Ring Systems, Molecular Crystals and Liquid Crystals, 70:1, 289-300

To link to this article: http://dx.doi.org/10.1080/00268948108073595

Mol. Cryst. Liq. Cryst., 1981, Vol. 70, pp. 289–300
0026-8941/81/7001-0289 $06.50/0

Physical Properties of Nematic Materials Containing Different Ring Systems†

M. J. BRADSHAW, D. G. McDONNELL and E. P. RAYNES
Royal Signals and Radar Establishment, Malvern, Worcs, WR14 3PS, UK

(*Received November 26, 1980*)

Measurements of the elastic constants, dielectric permittivities, refractive indices, order parameter, viscosity, and electro-optic properties are reported on mixtures of nematic materials containing terminal cyano groups and phenyl, trans-1,4-disubstituted cyclohexane, and bicyclo(2,2,2) octane rings.

INTRODUCTION

The application of liquid crystals to display devices makes demands on the properties of these materials far in excess of the initial desire for a wide temperature range and stability. The detailed electro-optic properties of materials in display devices, particularly the twisted nematic display, are now important. Consequently specific requirements exist for various physical properties such as the refractive indices, viscosity, dielectric permittivities, and elastic constants. Traditionally liquid crystals contain phenyl rings, and the replacement of the phenyl ring in a liquid crystal by other ring systems affords a convenient method of changing these physical properties. We have therefore studied the effect on physical properties of the replacement of a phenyl ring in the 4′-*n*-alkyl-4-cyanobiphenyls (CB)[1] by a trans-1,4-disubstituted cyclohexane ring (PCH),[2] and by a bicyclo(2,2,2)octane ring (BCO).[3] Measurements were made over a large temperature range by using mixtures of the three homologues R = n-C_3H_7, n-C_5H_{11}, and n-C_7H_{15}; in each case the mixture contained 30%, 40% and 30% by weight of the three homologues respec-

---

† Paper presented at the Eighth International Liquid Crystal Conference, Kyoto, Japan, June 30–July 4, 1980.

tively, and although none of the mixtures was eutectic, all were adequately close. The structures of the three systems and the nematic ranges of the mixtures are shown in Table I.

REFRACTIVE INDICES

The ordinary (n_0) and extraordinary (n_e) refractive indices were measured to an accuracy of 0.01% at 589.6 nm (D_1 sodium line) using an Abbé Refractometer. The prisms were coated with lecithin to induce homeotropic alignment; this allowed the measurement of n_0 and n_e directly in the same experiment.

The refractive indices of the nematic phase (n_0, n_e) and the isotropic phase ($n_{\text{isotropic}}$) as a function of reduced temperature are shown in Figure 1. The re-

TABLE I

Nematic range of 3/5/7 mixtures (°C)

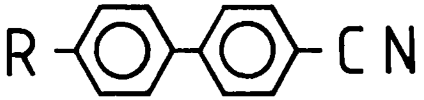	-10 → 35
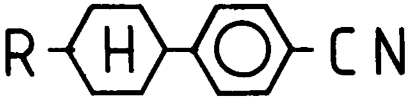	0 → 50
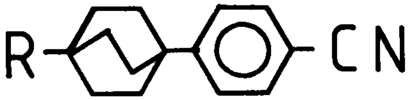	20 → 92

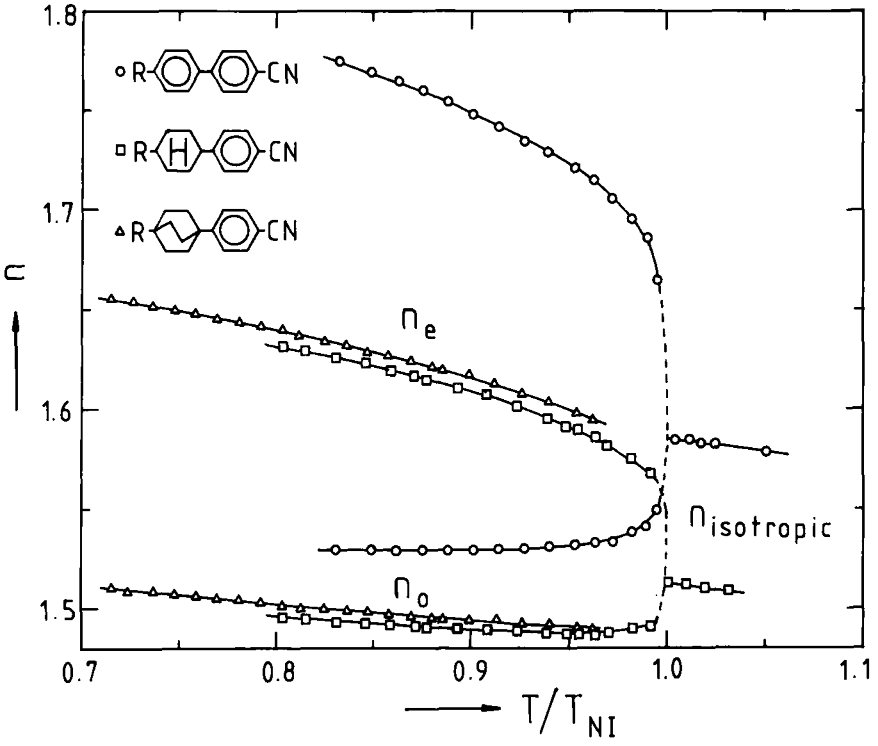

FIGURE 1 Refractive indices in the nematic and isotropic phases.

fractive indices and the birefringences ($\Delta n = n_e - n_o$) of the PCH and BCO mixtures are similar, whereas both n_e and Δn of the CB mixture are larger. This difference can be attributed to the larger contribution to the mean molecular polarizability ($\bar{\alpha}$) and the polarizability anisotropy ($\Delta\alpha$) of the phenyl ring compared with either of the saturated rings. The larger birefringence of the CB mixture ($\Delta n \approx 0.25$) allows twisted nematic (TN) devices as thin as 6 μm to be constructed without the appearance of color fringes, whereas the two saturated systems show a lower birefringence ($\Delta n \approx 0.15$) and must therefore be used in thicker (10 μm) TN devices.

The refractive indices have also been analyzed following the method of Haller[4] to give the order parameter S of the nematic phase. This method uses the Vuks[5] relation

$$S(\Delta\alpha/\bar{\alpha}) = (\bar{n}_e^2 - n_o^2)/(\bar{n}^2 - 1)$$

where

$$\bar{n}^2 = (n_e^2 + 2n_o^2)/3$$

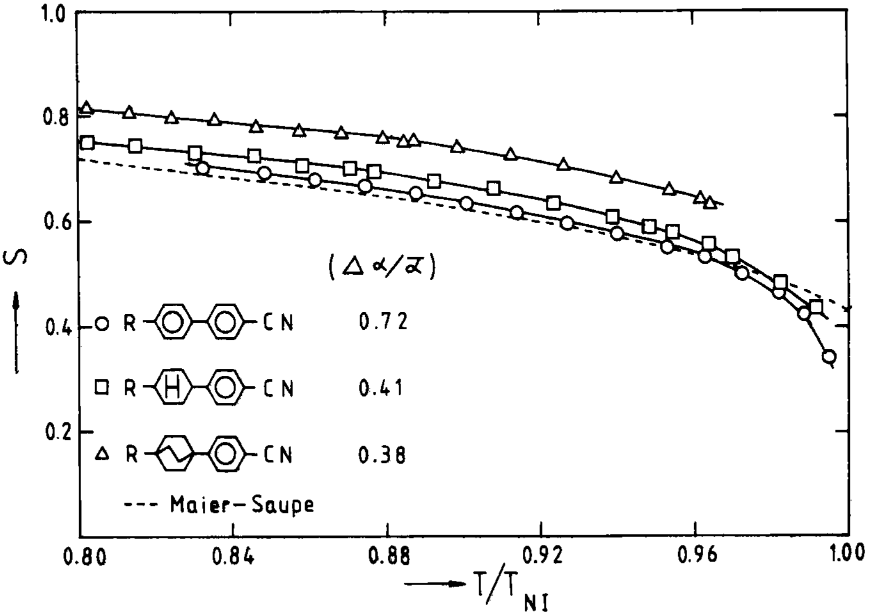

FIGURE 2 Order parameters and $(\Delta\alpha/\bar{\alpha})$ deduced from the refractive indices.

together with a simple extrapolation to $T = 0$ (where $S = 1$) to obtain $(\Delta\alpha/\bar{\alpha})$. The measured order parameters are shown in Figure 2 together with the mean field Maier-Saupe value and the values of $(\Delta\alpha/\bar{\alpha})$. The magnitude of S shows an increase in going from CB to PCH to BCO, and all are somewhat higher than the Maier-Saupe curve (except for close to T_{NI}). The reduced temperature dependence of S

$$-(dS/dT)/S$$

has also been calculated from the data. This does not depend on the fitted value of $(\Delta\alpha/\bar{\alpha})$, and is therefore more accurate. Typical results are given for $T/T_{NI} = 0.9$ in Table II and show that there is a steady lowering from 0.69%/°C for CB to 0.59%/°C for PCH to 0.40%/°C for BCO.

VISCOSITIES

The bulk viscosities were measured using a Brookfield rotating cone viscometer to an accuracy of 3%. Figure 3 shows the viscosities plotted against $(1/T)$, with the linear portions showing that away from the clearing point, the viscosity ($\bar{\eta}$) is given by the usual expression

$$\bar{\eta} = \bar{\eta}_0 \exp(Ea/kT)$$

where *Ea* is the activation energy.

Although the magnitudes of the viscosities of CB and PCH are similar, differing by only 15% at 0° C (which is well below the influence of T_{NI}), that of the

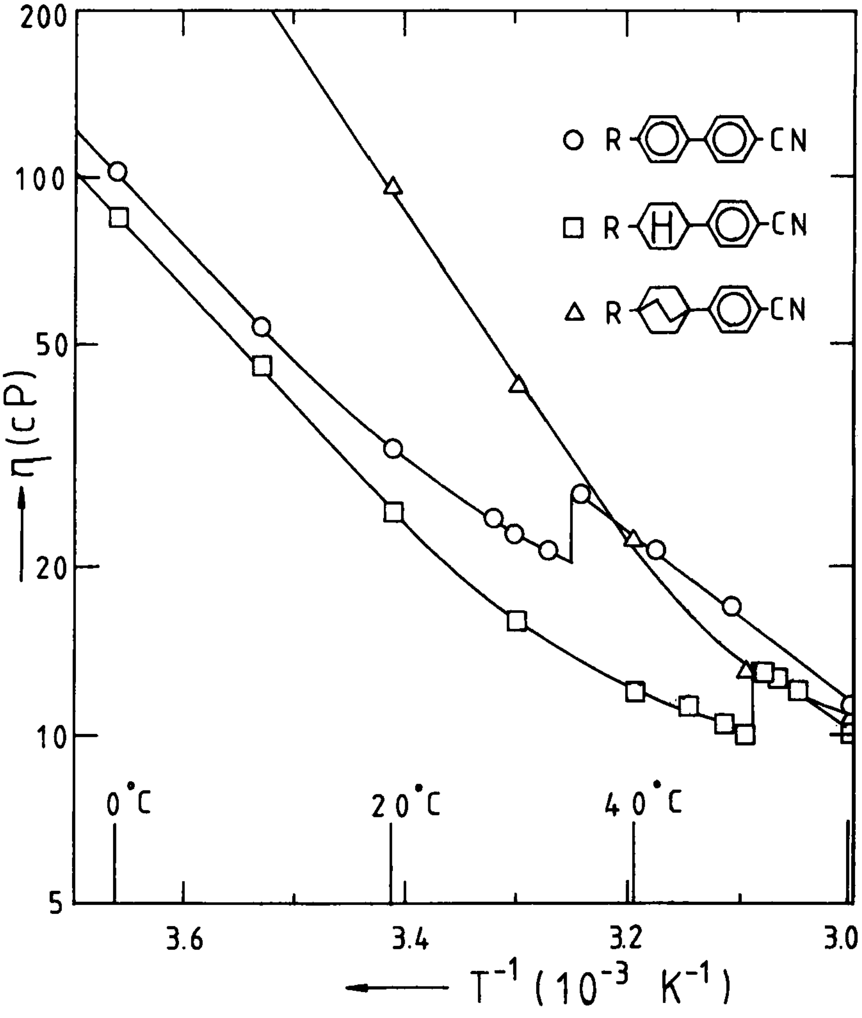

FIGURE 3 Bulk viscosities plotted against the reciprocal of absolute temperature.

BCO is significantly higher. Analysis of the viscosity data shows similar values for the activation energies of CB and PCH in both the nematic and isotropic phases and a significantly higher activation energy for BCO in the nematic phase.

DIELECTRIC PERMITTIVITIES

The dielectric permittivity components parallel and perpendicular to the director ($\epsilon_{\parallel}$ and $\epsilon_{\perp}$) were determined to within 0.5% from the capacitance of a parallel plate capacitor measured empty and then full of liquid crystal using an experimental technique described fully elsewhere.[6] A layer of "silicon monoxide" 100 Å thick and evaporated at 60° to the plate normal was used to induce an initial homogeneous alignment. The capacitance in a low electric field gave $\epsilon_{\perp}$ directly, and an extrapolation procedure[6] was used to estimate $\epsilon_{\parallel}$ from the high field data.

The permittivity components are plotted against reduced temperature in Figure 4 together with the mean $\bar{\epsilon} = (\epsilon_{\parallel} + 2\epsilon_{\perp})/3$ and isotropic ($\epsilon_{\text{isotropic}}$) values. The CB mixture shows the largest values of the permittivities ($\epsilon_{\perp}$, $\epsilon_{\parallel}$, and $\bar{\epsilon}$), with PCH and BCO having similar but lower values. The larger permittivities of CB arise from a greater contribution to the dipole moment induced

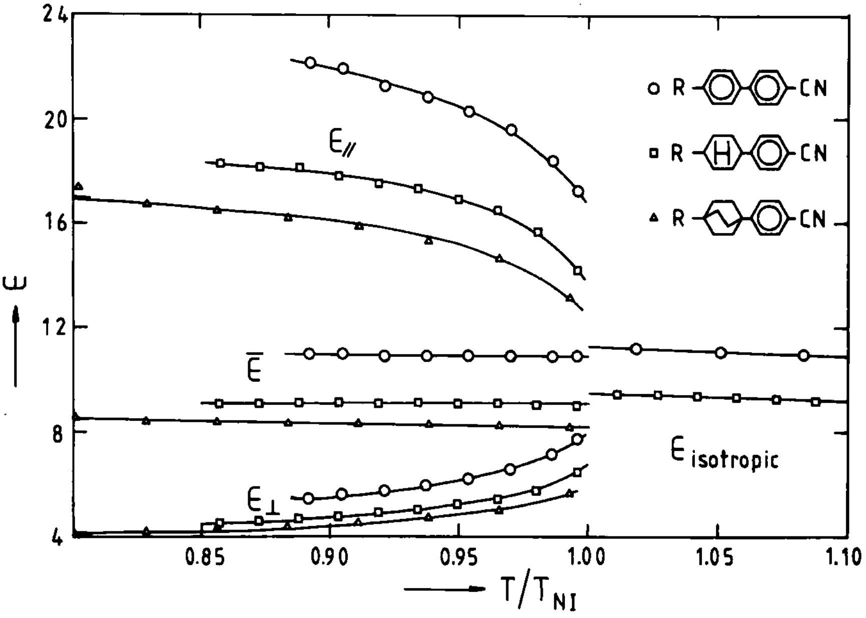

FIGURE 4 Dielectric permittivities in the nematic and isotropic phases.

by the cyano group adjacent to the two unsaturated phenyl rings. Specifically we note that the dielectric anisotropy ($\Delta\epsilon = \epsilon_{\parallel} - \epsilon_{\perp}$) is larger for CB, producing lower threshold voltages in field effect devices.

For all three mixtures $\bar{\epsilon}$ is virtually independent of temperature and is discontinuous with $\epsilon_{\text{isotropic}}$ at T_{NI}. These two factors are indicative of the strong anti-parallel ordering of molecules found in cyano systems.[7]

ELASTIC CONSTANTS

The splay, twist, and bend elastic constants (k_{11}, k_{22} and k_{33}) were determined from the detailed capacitance-voltage curves obtained using the same experimental technique as described in the previous section.[6] The capacitance-voltage curve for a parallel aligned cell (no twist) was analyzed by a non-linear least squares fitting program[8] to give k_{11} and k_{33} to an accuracy of 2% and 5% respectively. The twist elastic constant k_{22} was determined to within 10% from the threshold voltage of a 90° twist cell, estimated from its capacitance-voltage curve just above threshold.

The data are presented as k_{11} (Figure 5), and as the ratios k_{33}/k_{11} (Figure 6)

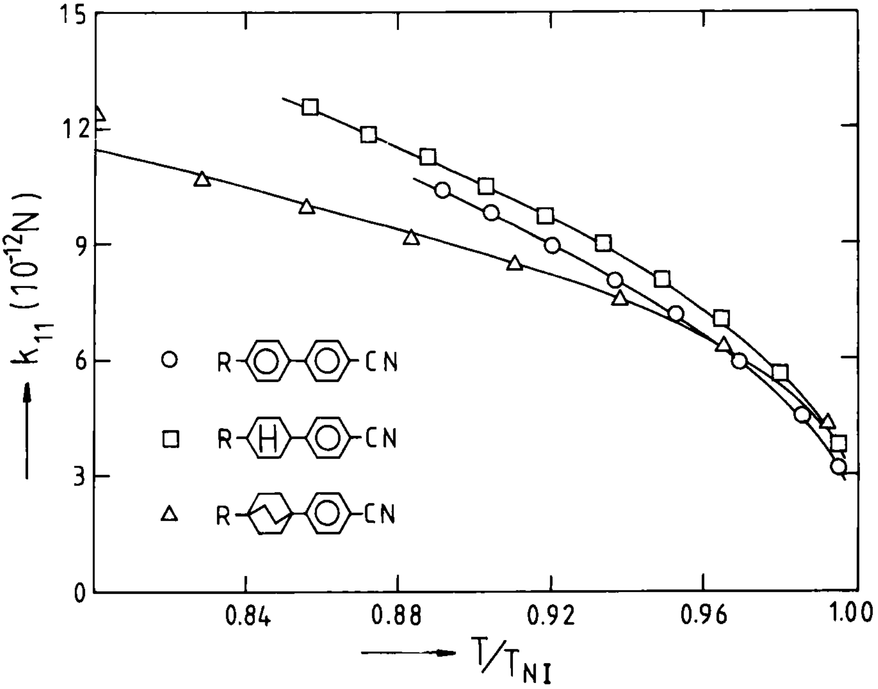

FIGURE 5 Splay elastic constants (k_{11}) against reduced temperature.

and k_{22}/k_{11} (Figure 7), all being plotted against reduced temperature. The values of (k_{33}/k_{11}) shown in Figure 6 show significant differences between the three ring systems, with CB showing the lowest value of k_{33}/k_{11} and BCO the highest. The value for BCO approaches 3, a surprisingly high value. This is in no way associated with the formation of a smectic phase, as the BCO mixture remains nematic at low temperatures. Large values of k_{33}/k_{11} have also been observed in recent studies on single BCO components. The ratio K_{22}/k_{11} is shown in Figure 7, and generally shows smaller effects due to the three ring systems.

The elastic constants and order parameters have been compared with the mean field theory of Priest[9] and the continuum theory of Faber.[10] Priest's theory was tested by using the combinations of k_{11}, k_{22}, and k_{33} suggested by Bunning *et al.*[11]

$$1/7(4k_{11} + 3k_{33}) = \bar{k}(1 + \Delta) = AS^2(1 + \Delta)$$
$$1/7(k_{33} - k_{11}) + k_{22} = \bar{k}(1 - 2\Delta) = AS^2(1 - 2\Delta)$$

where

$$\bar{k} = (k_{11} + k_{22} + k_{33})/3 = AS^2$$

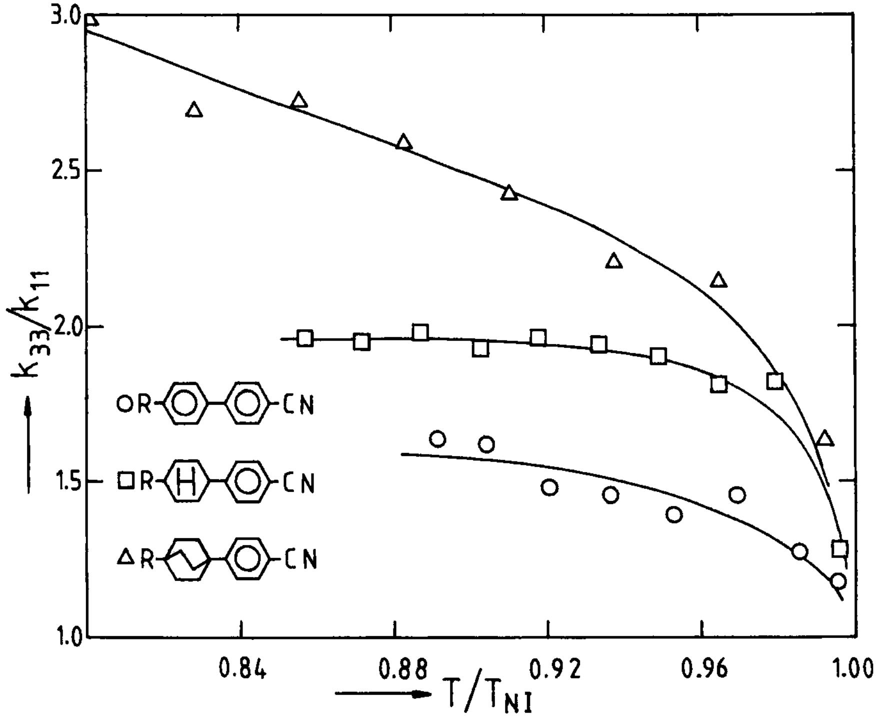

FIGURE 6 Ratio of bend/splay elastic constants (k_{33}/k_{11}).

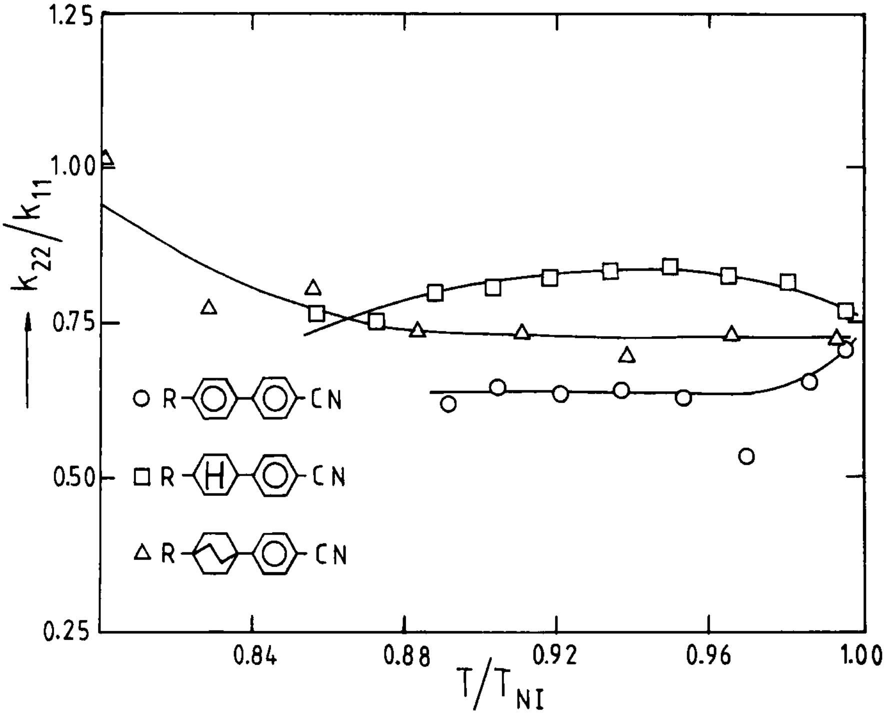

FIGURE 7 Ratio of twist splay elastic constants (k_{22}/k_{11}).

The logarithmic plots were all linear with slopes ≈ 2. However a companion logarithmic plot of $\bar{k}$ against S did not show the $\bar{k}\alpha S^2$ dependence for the BCO and CB mixtures, and therefore the preceding linear behavior must be regarded as fortuitous.

Faber's theory was tested by plotting T/k_F against $\ln S$, where

$$2/k_F = [k_{22}(k_{33} - k_{22})]^{-1/2} \arctan\left(\frac{k_{33} - k_{22}}{k_{22}}\right)^{1/2} + [k_{11}(k_{33} - k_{11})]^{-1/2} \arctan\left(\frac{k_{33} - k_{11}}{k_{11}}\right)^{1/2}$$

All three materials showed linear plots, with intercepts at $T = 0$ of $S = 0.82$, 0.95, and 0.96 respectively for CB, PCH, and BCO. None of the materials showed the unique slope predicted by Faber.

Therefore conclusive agreement cannot be found with the theories of either Priest or Faber. In fact, the best agreement is obtained with the simple mean field prediction of Nehring and Saupe[12] that $k_{11}\alpha S^2$ (Figure 8), although it

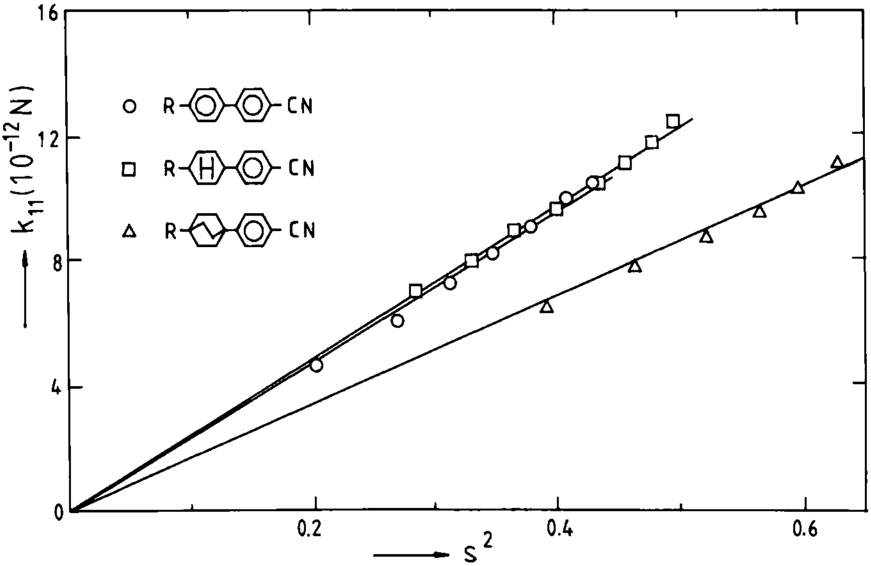

FIGURE 8 Splay elastic constants (k_{11}) against square of order parameter (S^2).

should be noted that their prediction for the ratios k_{22}/k_{11} and k_{33}/k_{11} do not agree with our results. This proportionality allows for a simple and quantitatively correct explanation of the different temperature dependences of k_{11} (Table II) in terms of the different temperature dependences of the order parameter *via* the relation

$$(1/k_{11})dk_{11}/dT = (2/S)(dS/dT)$$

ELECTRO-OPTIC PERFORMANCE IN TN DEVICES

The electro-optic performances of the materials were assessed in TN devices measured in transmission using a method described elsewhere.[13] It is not obvious if it is best to measure the materials using cells of the same thickness (d), or optical thickness ($d\Delta n$). To cover both options CB ($\Delta n \approx 0.25$) was measured using both 6 μm and 12 μm devices, and PCH and BCO (both $\Delta n \approx 0.15$) using 12 μm devices. Table II summarizes the data on temperature dependences and steepness measured at $T = 0.9T_{NI}$ as well as response times measured at 0° C.

The temperature dependence of the threshold voltage at 45° incidence V_{90} (45°) (for nomenclature see Ref. 13) is lowest for BCO and highest for CB. This reflects the trend in $(1/k_{11})dk_{11}/dT$, which in turn is related to the trend in $(1/S)dS/dT$. The low temperature dependence of BCO makes them of interest

TABLE II

Electro-optic and other relevant properties

Property (at $T = 0.9\ T_{NI}$) / Material	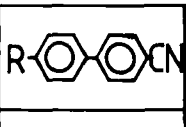			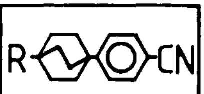
	6 µm	12 µm	12 µm	12 µm
$-\frac{1}{V_c}\left(\frac{dV_c}{dT}\right)^{(1)}$ (% / °C)	1.21	1.21	0.79	0.51
$-\frac{1}{k_{11}}\left(\frac{dk_{11}}{dT}\right)$ (% / °C)	1.49		1.23	0.90
$-\frac{1}{S}\left(\frac{dS}{dT}\right)$ (% / °C)	0.69		0.59	0.40
$M_{0.9T_{NI}}$ (2)	1.90	1.97	1.91	1.97
$(5k_{33}/8k_{11} + \Delta\epsilon/\epsilon_\perp)$	3.87		3.91	4.06
T_{decay} (0 °C) (mS)	140	340	280	1300
Response factor(3) (0 °C) (P)	20		50	230

1 $V_c = V_{90}(45°)$

2 $M_{0.9T_{NI}} = V_{10}(0°)/V_{90}(45°)$

3 Response factor $= \eta/\Delta n^2$

for use in multiplexed TN displays operating over a range of temperature without temperature compensation of the drive voltages.

The steepness factor $M_{0.9T_{NI}}$[13] (measured at $T = 0.9\ T_{NI}$) shows a less clear trend. Although k_{33}/k_{11} increases from CB to PCH to BCO, this increase is somewhat masked by the corresponding decrease in $\Delta\epsilon/\epsilon_\perp$. Accordingly the appropriate combination $(5k_{33}/8k_{11} + \Delta\epsilon/\epsilon_\perp)$[14] is also shown in Table II, and is found to correlate more closely with the steepness factor. The larger steepness factor (and k_{33}/k_{11}) of BCO makes them less attractive for multiplexed TN displays; however the overall suitability for multiplexed TN displays involves a combination of low temperature dependence and good steepness. It is not therefore clear at this stage which of CB, PCH, and BCO is the most suitable for multiplexed TN displays. It seems likely that the choice will depend on the specific requirements and may even involve combinations of materials.

The decay times measured at 0° C illustrate clearly the predicament in the choice of cell spacing. In the 12 μm devices there is an obvious correlation with the viscosities reported earlier, with PCH having the lowest value. However, the larger Δn of CB allows operation in a 6 μm device, which shows by far the quickest response time. It therefore seems reasonable to consider the "response factor" given by $\eta / \Delta n^2$ as a measure of the ultimate response time of the material in the thinnest device allowed by the Mauguin limit. The response factor shows reasonable correlation with the decay time measured for CB using 6 μm layers, and PCH and BCO using 12 μm layers.

Acknowledgments

We wish to thank George Gray and Stephen Kelly of Hull University, BDH Chemicals Ltd, and E. Merck for supply of the materials, and Anne Mayo for technical assistance.

References

1. G. W. Gray, K. J. Harrison and J. A. Nash, *Electron. Lett.*, **9**, 130 (1973).
2. R. Eidenschink, D. Erdmann, J. Krause and L. Pohl, *Angew. Chem.*, **89**, 103 (1977).
3. G. W. Gray and S. M. Kelly, *Angew. Chem.*, in press.
4. (a) I. Haller, *Prog. Solid-State Chem.*, **10**, 103 (1975). (b) R. G. Horn, *J. Phys. (Paris)*, **39**, 105 (1978).
5. M. F. Vuks, *Opt. and Spectrosc.*, **20**, 361 (1966).
6. M. G. Clark, E. P. Raynes, R. A. Smith and R. J. A. Tough, *J. Phys. D: Appl. Phys.*, in press.
7. N. V. Madhusudana and S. Chandrasekhar, in Proceedings of the International Liquid Crystals Conference, Bangalore, December 1973, Pramana Supplement I, p. 57.
8. R. J. A. Tough and E. P. Raynes, *Mol. Cryst. Liq. Cryst. Lett.*, **56**, 19 (1979).
9. R. G. Priest, *Phys. Rev.*, **A7**, 720 (1973).
10. T. E. Faber, *Proc. Roy. Soc. Lond.*, **A353**, 247 (1977).
11. J. D. Bunning, T. E. Faber and P. L. Sherrell, *J. Phys. (Paris)*, in press.
12. J. Nehring and A. Saupe, *J. Chem. Phys.*, **56**, 5527 (1972).
13. E. P. Raynes, *IEEE Trans. Electron. Devices*, **ED-26**, 1116 (1979).
14. E. P. Raynes, R. J. A. Tough and K. A. Davies, *Mol. Cryst. Liq. Cryst. Lett.*, **56**, 63 (1979).